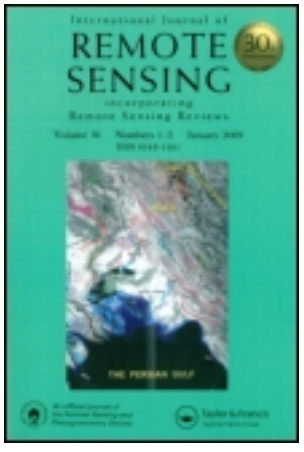

International Journal of Remote Sensing

Publication details, including instructions for authors and subscription information:
http://www.tandfonline.com/loi/tres20

Modelling gross primary production of a tropical semi-deciduous forest in the southern Amazon Basin

Marcelo Sacardi Biudes[a], Maísa Caldas Souza[a], Nadja Gomes Machado[ab], Victor Hugo de Morais Danelichen[a], George Louis Vourlitis[c] & José de Souza Nogueira[a]

[a] Programa de Pós-Graduação em Física Ambiental, Instituto de Física, Universidade Federal de Mato Grosso, Cuiabá, Mato Grosso, Brazil

[b] Laboratório da Biologia da Conservação, Instituto Federal de Mato Grosso - Campus Bela Vista, Cuiabá, Mato Grosso, Brazil

[c] Biological Sciences Department, California State University, San Marcos, California, USA

Published online: 17 Feb 2014.

To cite this article: Marcelo Sacardi Biudes, Maísa Caldas Souza, Nadja Gomes Machado, Victor Hugo de Morais Danelichen, George Louis Vourlitis & José de Souza Nogueira (2014) Modelling gross primary production of a tropical semi-deciduous forest in the southern Amazon Basin, International Journal of Remote Sensing, 35:4, 1540-1562, DOI: 10.1080/01431161.2013.878059

To link to this article: http://dx.doi.org/10.1080/01431161.2013.878059

International Journal of Remote Sensing, 2014
Vol. 35, No. 4, 1540–1562, http://dx.doi.org/10.1080/01431161.2013.878059

Taylor & Francis
Taylor & Francis Group

Modelling gross primary production of a tropical semi-deciduous forest in the southern Amazon Basin

Marcelo Sacardi Biudes[a], Maísa Caldas Souza[a], Nadja Gomes Machado[a,b], Victor Hugo de Morais Danelichen[a], George Louis Vourlitis[c]*, and José de Souza Nogueira[a]

[a]*Programa de Pós-Graduação em Física Ambiental, Instituto de Física, Universidade Federal de Mato Grosso, Cuiabá, Mato Grosso, Brazil;* [b]*Laboratório da Biologia da Conservação, Instituto Federal de Mato Grosso – Campus Bela Vista, Cuiabá, Mato Grosso, Brazil;* [c]*Biological Sciences Department, California State University, San Marcos, California, USA*

(*Received 26 February 2013; accepted 7 December 2013*)

Semi-deciduous forest in the Amazon Basin is sensitive to temporal variation in surface water availability that can limit seasonal rates of leaf and canopy gas exchange. We estimated the seasonal dynamics of gross primary production (GPP) over 3 years (2005–2008) using eddy covariance and assessed canopy spectral reflectance using MODIS imagery for a mature tropical semi-deciduous forest located near Sinop, Mato Grosso, Brazil. A light-use efficiency model, known as the Vegetation Photosynthesis Model (VPM), was used to estimate seasonal and inter-annual variations in GPP as a function of the enhanced vegetation index (EVI), the land surface water index (LSWI), and local meteorology. Our results indicate that the standard VPM was incapable of reproducing the seasonal variation in GPP, primarily because the model overestimated dry-season GPP. In the standard model, the scalar function that alters light-use efficiency (ε_g) as a function of water availability (W_{scalar}) is calculated as a linear function of the LSWI derived from MODIS; however, the LSWI is negatively correlated with several measures of water availability including precipitation, soil water content, and relative humidity (RH). Thus, during the dry season, when rainfall, soil water content, and RH are low, LSWI, and therefore, W_{scalar}, are at a seasonal maximum. Using previous research, we derived new functions for W_{scalar} based on time series of RH and photosynthetic photon flux density (PPFD) that significantly improved the performance of the VPM. Whether these new functions perform equally well in water stressed and unstressed tropical forests needs to be determined, but presumably unstressed ecosystems would have high cloud cover and humidity, which would minimize variations in W_{scalar} and GPP to spatial and/or temporal variation in water availability.

1. Introduction

Tropical forests have received special attention because they have extremely high biodiversity (Losos and Leigh 2004), account for 40% of net primary productivity (NPP) and 30% of all terrestrial carbon stored in biomass (Saatchi et al. 2011), and have been severely impacted by land-use and land-cover change (Nepstad et al. 2008; Davidson et al. 2012). Brazil has one of the largest expanses of rainforest of the world, and contains approximately 20% of the global carbon store (Bernoux et al. 2002). However, conversion of forest to pasture and/or cropland released approximately 0.7–1.4 PgC year^{-1} to the atmosphere between 1996 and 2005 (Houghton 2005). It is estimated that the Amazon forest will be reduced to half the original

*Corresponding author. Email: georgev@csusm.edu

size by 2030, which can modify the regional climate and impact ecosystem functioning (Laurance 2006; Nepstad et al. 2008). Recent analyses suggest that the sink strength of the Amazon Basin has declined over the last two decades, perhaps because of an intensification of the dry season (Gloor et al. 2012). Quantifying the magnitude and temporal dynamics of net terrestrial C exchange is essential for understanding the ecosystem functioning of Amazon rainforest (Hutyra et al. 2007; Vourlitis et al. 2011; Kim et al. 2012).

Studies relying on satellite-based remote sensing indicate that canopy greenness in the Amazon forest is negatively correlated with precipitation patterns, resulting in higher productivity during the dry season (Saleska et al. 2003; Huete et al. 2006; Myneni et al. 2007; Hutyra et al. 2007; Davidson et al. 2012). These seasonal patterns are thought to be due to a stronger light limitation to primary production than water during the dry season, when radiation is at a seasonal maximum (Saleska et al. 2003, 2009; Hutyra et al. 2007). However, this pattern is not general to the Amazon Basin, and in particular, forests in the southern part of the basin reportedly experience either no increase or a decline in productivity during the dry season in response to drought (Samanta et al. 2010; Zhao and Running 2010; Vourlitis et al. 2011). In particular, semi-deciduous forests in the southern Amazon Basin, which occupy a climatic transition between humid tropical forest and savanna, experience high annual precipitation but with distinct wet and dry seasons (da Rocha et al. 2009; Vourlitis et al. 2004, 2008). Seasonal drought has been shown to limit leaf gas exchange (Miranda et al. 2005; Sendall, Vourlitis, and Lobo 2009), gross primary production (GPP), and soil and whole-ecosystem respiration (Valentini et al. 2008; Vourlitis et al. 2004, 2005, 2011); and in many respects, seasonal variations in water and net CO_2 exchange of these forests more closely resemble those reported for savanna than the Amazonian forest (Meir et al. 2008; Vourlitis and da Rocha 2010). These large spatial variations highlight the complex interactions between drought, phenology, and productivity across the Amazon Basin (Saleska et al. 2009), and the need to link ground-based and remotely based observations of surface biophysical phenomena to understand basin-wide variations in forest function (Silva et al. 2013).

Recently, the Vegetation Photosynthesis Model (VPM) was developed (Xiao, Hollinger, et al. 2004; Xiao, Zhang, et al. 2004) to predict light absorption by chlorophyll and GPP of terrestrial ecosystems, based on the concept that the vegetation canopy is composed of chlorophyll and non-photosynthetically active vegetation (NPV). The VPM has been used to predict GPP for flux tower sites in temperate deciduous broadleaf forest (Xiao, Hollinger, et al. 2004; Xiao, Zhang, et al. 2004), Amazonian tropical forest (Xiao et al. 2005), and croplands (Li et al. 2007; Wang, Xiao, and Yan 2010). Here, we extend these analyses to the semi-deciduous forest of the southern Amazon Basin to determine the effectiveness of the VPM to explain the observed seasonal and inter-annual variations in GPP and to understand the underlying biophysical mechanisms for these variations. Our objectives were to evaluate (i) links between vegetation indices derived from MODIS land-surface reflectance and ground-based measurements of forest structure and function, and (ii) the potential of VPM for estimating GPP of an Amazon–savanna transitional forest. We hypothesize that (i) seasonal and/or inter-annual drought will be the primary factor in limiting GPP and canopy greenness and that (ii) the VPM will provide accurate seasonal and inter-annual estimates of GPP for these tropical, semi-deciduous forests.

2. Materials and methods

2.1. Site description

The study was conducted between July 2005 and June 2008 in a semi-deciduous forest located 50 km northeast of Sinop, Mato Grosso, Brazil (11° 24.75′ S: 55° 19.50′ W;

423 m above sea level). The area is in a climatic transition between humid tropical forest to the north and savanna to the south and east. The forest canopy is on average 25–28 m tall with 94 species ha^{-1} and 35 plant families ha^{-1} of woody trees and vines ≥10 cm in diameter; however, more than 50% of all trees are composed of *Protium sagotianum* Marchland (Burseraceae), *Tovomita schomburgkii* Planch & Triana (Clusiaceae), *Brosimum lactescens* (S. Moore) C.C. Berg (Moraceae), and *Dialium guianense* (Aubl.) Sandwith (Caesalpiniaceae) (Sanches et al. 2008). The mean basal area of woody plants was 22.5 m^2 ha^{-1} and the density was 483 stems ha^{-1}, with 60% of all individuals belonging to the 10–20 cm diameter size class (Sanches et al. 2008). The leaf area index (LAI) varies from 7–8 m^2 m^{-2} in the wet season to 6–7 m^2 m^{-2} in the dry season (Biudes et al. 2013). The soil is a quartzarenic neosol characterized by ~90% sand, low pH (4.2), and low fertility (Almeida 2005). The climate is classified as Aw according to Köppen, with a 30 year mean annual temperature of 24°C and annual rainfall of 2037 mm, and a distinct dry season from May to September (Vourlitis et al. 2008, 2011).

2.2. *Eddy covariance and micrometeorological measurements*

Net ecosystem exchange (NEE) and energy balance were measured using the eddy covariance method. Eddy covariance sensors were mounted on a walk-up tower at a height of 42 m above ground level or 14–17 m above the forest canopy (Vourlitis et al. 2011). The eddy covariance system utilized a three-dimensional sonic anemometer-thermometer (CSAT-3, Campbell Scientific, Inc., Logan, UT, USA) to measure the mean and fluctuating quantities of wind speed and temperature and an open-path infrared gas analyser (LI-7500, LI-COR, Inc. Lincoln, NE, USA) to measure the mean and fluctuating quantities of H_2O vapour and CO_2 molar density. The infrared gas analyser was installed approximately 5 cm downwind of the sonic anemometer to minimize sensor separation and at an angle of 20° to allow moisture from rain or dew to rapidly roll-off the light-source window. Raw (10 Hz) and average CO_2 and H_2O vapour fluxes data were stored and processed using a solid-state data logger (CR5000, Campbell Scientific, Inc., Logan, UT, USA).

Canopy CO_2 storage was determined by quantifying the rate of change of the CO_2 concentration of the air column between the ground surface and the eddy covariance sensors (Grace et al. 1996; Vourlitis et al. 2011). Air samples were drawn at 1, 4, 12, 20, and 28 m above the ground level using a diaphragm pump and solenoid switching system, and the vertical CO_2 concentration profile was measured using a closed-path CO_2 analyser (LI-820, LI-COR, Inc., Lincoln, NE, USA). The gradient measurement system was operational for 30% of all the observations, and during system failure canopy CO_2 storage was quantified from the CO_2 concentration measurements made at the top of the tower (Hollinger et al. 1994), which did not differ from those derived from the gradient measurements (Vourlitis et al. 2011).

Photosynthetic photon flux density (PPFD) was measured above the canopy (40 m above ground level) using a quantum sensor (LI-190SB, LI-COR, Lincoln, NE, USA). The air temperature and relative humidity (RH) were measured at the top of the tower using a thermohygrometer (HMP-45 C, Vaisala Inc., Helsinki, Finland). Micrometeorological sensor output was measured every 30 s using a solid-state data logger (CR5000, Campbell Scientific, Inc., Logan, UT, USA) and data were averaged over half-hourly intervals. Precipitation data were obtained daily from a manual rainfall gauge located 5 km southeast of the eddy flux tower because data obtained at the eddy flux tower was periodically unavailable and/or unreliable. These data were highly

correlated with data collected on-site, with a mean (±95% CI) linear regression slope of 0.98 ± 0.18 and y-intercept that was not significantly different from zero ($r^2 = 0.91$; $n = 7$ months; Vourlitis et al. 2008, 2011).

2.3. CO_2 flux calculation and data treatment

Carbon dioxide and energy fluxes were obtained by calculating the covariance between the fluctuations in vertical wind speed and fluctuations in virtual temperature, H_2O vapour, or CO_2 molar density following a coordinate rotation of the wind vectors (McMillen 1988) and averaged over 30 min time periods. Eddy CO_2 flux derived from the open-path gas analyser was corrected for simultaneous fluctuations in heat and H_2O vapour whereas eddy H_2O vapour flux was corrected for fluctuations in heat flux (Webb, Pearman, and Lenning 1980).

NEE was calculated as the sum of eddy CO_2 flux and canopy CO_2 storage. NEE data were screened for quality following guidelines established by Ameriflux and Anthoni, Law, and Unsworth (1999). Data were rejected when (1) eddy covariance sensors failed or were down because of calibration and system maintenance, (2) warming flags were generated by the system software indicating measurement and/or processing errors, (3) spikes in sonic and/or infrared gas analyser data were excessive, such as during heavy rainfall events, (4) abrupt changes in wind speed caused non-stationary conditions, and (5) eddy flux data were outside physically and/or biologically meaningful ranges. With instrument malfunction, weather variation, and calibration issues, 66–75% of all possible CO_2 flux data were obtained, and 78–91% of all possible micrometeorological data were obtained (Vourlitis et al. 2011).

GPP was estimated by Equation (1) following the methods described by Wohlfahrt et al. (2005):

$$\mathrm{GPP} = \mathrm{NEE} \quad R_{\mathrm{eco}}, \tag{1}$$

where NEE is the daytime (PPFD > 5 μmol photons m^{-2} s^{-1}) net ecosystem CO_2 exchange measured from eddy covariance and R_{eco} is an average rate of daytime ecosystem respiration. Daytime R_{eco} and GPP were derived using a Michaelis–Menton-type function (Ruimy et al. 1995; Wohlfahrt et al. 2005) by Equation (2) over 8 day intervals (to be consistent with MODIS data acquisition described below):

$$\mathrm{NEE} = \frac{\varepsilon_0 Q_{\mathrm{PPFD}} F_{\mathrm{GPP,sat}}}{\varepsilon_0 Q_{\mathrm{PPFD}} + F_{\mathrm{GPP,sat}}} \quad R_{\mathrm{eco}}, \tag{2}$$

where ε_0 is the apparent quantum yield (μmol CO_2 μmol photons^{-1}), Q_{PPFD} is the measured average 30 min average PPFD (μmol photons m^{-2} s^{-1}), $F_{\mathrm{GPP,sat}}$ is the light-saturated rate of GPP (μmol CO_2 m^{-2} s^{-1}), and R_{eco} is the daytime respiration rate that is estimated as the intercept of Equation (2) where PPFD = 0 μmol photons m^{-2} s^{-1}. Estimates of R_{eco} derived using these methods compare well to those estimated from night-time data (Falge et al. 2001), and minimize problems associated with night-time flux loss from low turbulence and errors in objectively selecting a turbulence (i.e. frictional velocity) threshold that excludes data measured under inadequate turbulence (Wohlfahrt et al. 2005).

2.4. Satellite imagery and vegetation indices

We downloaded the 8 day composite land-surface reflectance data (MOD09A1) from the EROS Data Active Archive Center (EDC Daac, http://daac.ornl.gov/cgi-bin/MODIS/GLBVIZ_1_Glb/modis_subset_order_global_col5.pl) based on the geo-location information (latitude and longitude) of the eddy covariance flux tower from July 2005 to June 2008. The MOD09A1 data sets include seven spectral bands, at a spatial resolution of 500 m, and are corrected for the effects of atmospheric gases, aerosols, and thin cirrus clouds (Vermote and Kotchenova 2008). Land-surface reflectance values were averaged for the nine pixels covering and surrounding the eddy flux tower, and only pixels with highest quality assurance (QA) metrics were used.

Varying sensor-viewing geometry, cloud presence, aerosols, and bidirectional reflectance can limit the efficacy of reflectance data for assessing spatial–temporal dynamics in biophysical processes (Hird and McDermid 2009), and signal extraction techniques are often required to improve the signal–noise ratio (Hernance et al. 2007). Thus, we applied singular spectrum analysis (SSA) using CatMV software (Golyandina and Osipova 2007), which has been shown to be effective for the filtered reconstruction of short, irregularly spaced, and noisy time series (Ghil et al. 2002) and for improving the signal–noise ratio of the MODIS land-surface reflectance (Zeilhofer et al. 2011). SSA is initiated by the embedding of a time series $X(t)$: $t = 1, \ldots, N$ in a user-defined vector space of dimension M, to represent it as a trajectory in the phase space of the hypothetical system that generated $X(t)$ (Ghil et al. 2002). Using the Caterpillar method (Golyandina, Nekrutkin, and Zhigljavsky 2001), spectral information on the time series is obtained by diagonalizing the lag-covariance matrix $\mathbf{C}$ of $X(t)$. As a result of this decomposition, the M eigenvectors λk of the lag-covariance matrix $\mathbf{C}$ are called temporal empirical orthogonal functions (EOFs). The eigenvalues λk of $\mathbf{C}$ account for the partial variance in the direction, and the sum of the eigenvalues gives the total variance of the original time series $X(t)$. To reconstruct a filtered noise-reduced time series, eigenvalues that represent the signal (trend, periodicity) are selected. The Caterpillar method for time series with missing data was conducted using the CatMV software (Golyandina and Osipova 2007). For SSA filtering, a 1 year time window length was used for image decomposition (24 observations), with a threshold of 12 gaps (6 months) at maximum. Five EOFs (EVI: numbers 1, 8, 9, 23, and 24) were then applied for reconstruction. Comprehensive descriptions of SSA and the Caterpillar method are given in Golyandina, Nekrutkin, and Zhigljavsky (2001) and Golyandina and Osipova (2007).

Land-surface reflectance values from blue (ρ_{blue}), red (ρ_{red}), near-infrared (ρ_{nir}), and shortwave infrared (ρ_{swir}) were used to calculate the enhanced vegetation index (EVI) (Huete et al. 1997) and the land surface water index (LSWI) (Xiao et al. 2002; Xiao, Hollinger, et al. 2004). EVI has been used to characterize the seasonal variation of temperate (Xiao, Hollinger, et al. 2004a, 200b) and tropical forest (Xiao et al. 2005; Vourlitis et al. 2011) CO_2 exchange, and is superior to other indices for reducing atmospheric influences and characterizing dense vegetation (Huete et al. 2002), whereas the LSWI has been used to determine the potential for water stress in tropical forests by the leaf water content (Xiao et al. 2005). EVI utilizes red (ρ_{red}) and near-infrared bands (ρ_{nir}), and includes the blue band for atmospheric correction (Equation (3)) to account for residual atmospheric contamination (e.g. aerosols), variable soil, and canopy background reflectance (Huete et al. 1997), which is important in the Amazon Basin, particularly during the dry season, when smoke from biomass burning injects large amounts of particulates into the atmosphere:

$$\mathrm{EVI} = 2.5\frac{\rho_{\mathrm{nir}} \quad \rho_{\mathrm{red}}}{\rho_{\mathrm{nir}} + 6\rho_{\mathrm{blue}} \quad 7.5\rho_{\mathrm{red}} + 1}. \tag{3}$$

The shortwave infrared spectral band (ρ_{swir}) is sensitive to vegetation water content and soil moisture, and a combination of nir and swir bands have been used to derive the LSWI (Equation (4)):

$$\mathrm{LSWI} = \frac{\rho_{\mathrm{nir}} \quad \rho_{\mathrm{swir}}}{\rho_{\mathrm{nir}} + \rho_{\mathrm{swir}}}. \tag{4}$$

The swir absorption increases and swir reflectance decreases as leaf liquid water content increases or soil moisture increases, resulting in an increase of LSWI (Xaio et al. 2005).

2.5. *VPM and parameter estimation*

The VPM proposed by Xiao, Hollinger, et al. (2004), Xiao, Zhang, et al. (2004) is based on the concept that leaves and canopy are composed of photosynthetically active vegetation (PAV, mostly chloroplast) and non-photosynthetic vegetation (mostly senescent foliage, branches, and stems). The fraction of absorbed photosynthetically active radiation (FPAR) is partitioned into the fraction absorbed by chlorophyll ($\mathrm{FPAR_{chl}}$) and the fraction absorbed by NPV within the canopy ($\mathrm{FPAR_{NPV}}$). The predicted GPP (gC $\mathrm{m^{-2}}$ $\mathrm{day^{-1}}$) can be described by Equation (5) as follows:

$$\mathrm{GPP} = \varepsilon_g\,\mathrm{FPAR_{chl}}\,\mathrm{PPFD}, \tag{5}$$

where ε_g is the light-use efficiency (gC $\mathrm{molPPFD^{-1}}$) and $\mathrm{FPAR_{chl}}$ (Equation (6)) is the fraction of PPFD absorbed by chlorophyll. $\mathrm{FPAR_{chl}}$ is assumed to be a linear function of EVI (Xiao, Hollinger, et al. 2004; Xiao, Zhang, et al. 2004; Wang, Xiao, and Yan 2010); and following Xaio et al. (2005), who used the VPM to estimate the GPP of Amazonian forest near Santarem, Pará, we set the value of α = 1.0.

$$\mathrm{FPAR_{chl}} = \alpha\mathrm{EVI}. \tag{6}$$

ε_g (Equation (5)) is often considered to be a constant value that is parameterized based on prior knowledge from ground-based measurement campaigns (Wu et al. 2010). However, ε_g can vary as a function of meteorology and surface water availability, and previous research indicates that variations in ε_g may be large in tropical semi-deciduous forests, especially in response to phenology and water availability (Vourlitis et al. 2011). Variation in ε_g has been modelled as a function of a maximum value (ε_0) and scalar functions (Equation (7)):

$$\varepsilon_g = \varepsilon_0 T_{\mathrm{scalar}} W_{\mathrm{scalar}} P_{\mathrm{scalar}}, \tag{7}$$

where T_{scalar}, W_{scalar}, and P_{scalar} are the down-regulation scalars, ranging between 0 and 1, for the effects of temperature, water, and leaf phenology on light-use efficiency of vegetation, respectively, and ε_0 is the maximum apparent light-use efficiency estimated from the Michaelis–Menten function (Equation (2)) (Running et al. 2004; Xiao, Hollinger, et al. 2004; Xiao, Zhang, et al. 2004; Wu et al. 2010). We used a value of 0.54 gC $\mathrm{molPPFD^{-1}}$ for ε_0 to be consistent with that used by Xiao et al. (2005) for Amazonian forest; however, this value was comparable to the value of ε_0 that was estimated from our eddy covariance values of GPP.

We used scalar functions normally applied to these models to test their performance for our tropical semi-deciduous forest. T_{scalar} (Equation (8)) was developed for the Terrestrial Ecosystem Model (TEM) (Raich et al. 1991; Wu et al. 2010),

$$T_{scalar} = \frac{(T \quad T_{min})(T \quad T_{max})}{[(T \quad T_{min})(T \quad T_{max}) \quad (T \quad T_{opt})^2}, \tag{8}$$

where T is the air temperature at each time step (°C), and T_{min}, T_{max}, and T_{opt} are the minimum, maximum, and optimal temperature for photosynthetic activity (°C), respectively. If air temperature falls below T_{min}, T_{scalar} is set to zero. For tropical forest, T_{min} was set to 2°C, T_{opt} = 28°C, and T_{max} = 40°C, as reported by Doughty and Goulden (2008) and Vourlitis et al. (2011) and implemented in TEM (Raich et al. 1991; Wu et al. 2010). W_{scalar} (Equation (9)) represents the effect of water on plant photosynthesis, and has been estimated as a function of soil moisture, vapour pressure deficit (VPD), and, for our purposes, the satellite-derived water index (LSWI) (Running et al. 2000, Xiao, Hollinger, et al. 2004; Xiao, Zhang, et al. 2004, 2005):

$$W_{scalar} = \frac{1 + \mathrm{LSWI}}{1 + \mathrm{LSWI}_{max}}, \tag{9}$$

where LSWI_{max} is the maximum LSWI, which depends on the optical sensor and the time series of image data (Xiao, Hollinger, et al. 2004), and here, the maximum LSWI was observed during the early wet season and was equal to 0.38. P_{scalar} (Equation (10)) accounts for the effect of leaf phenology (leaf age) on canopy photosynthesis, and relies on LSWI to identify the green-up and senescence phase (Xiao, Zhang, et al. 2004; Wu et al. 2010). For a canopy that is dominated by leaves with a life expectancy of $\leq$1 year (e.g. deciduous trees), P_{scalar} is calculated as a linear function of LSWI at two different phases:

$$P_{scalar} = \frac{1 + \mathrm{LSWI}}{2}, \tag{10}$$

when leaves are expanding, and P_{scalar} = 1 after leaf expansion (Xiao, Zhang, et al. 2004; Wu et al. 2010).

3. Results and discussion

3.1. Seasonal variations in meteorology

Meteorological conditions varied substantially over the study period, with drier and warmer conditions during 2005–2006, wetter and warmer conditions during 2006–2007, and drier and cooler conditions during 2007–2008 (Vourlitis et al. 2011). Seasonal variations in air temperature were consistent from year to year, although air temperature was higher in 2005 (Figure 1(*a*)). Air temperature was generally lowest during the dry season, when the incursion of cold fronts to the southern portion of the Amazon Basin is more common (Machado et al. 2004), increased during the dry–wet season transition in August–September, and reached a peak during the early wet season in October. Average daily air temperature in October 2005 was approximately 2.5°C and 3°C higher than in 2006 and 2007, respectively, and this period is of particular interest because of intense drought reported throughout the southern Amazon Basin (Marengo et al. 2008). Wet season temperatures were more variable; however,

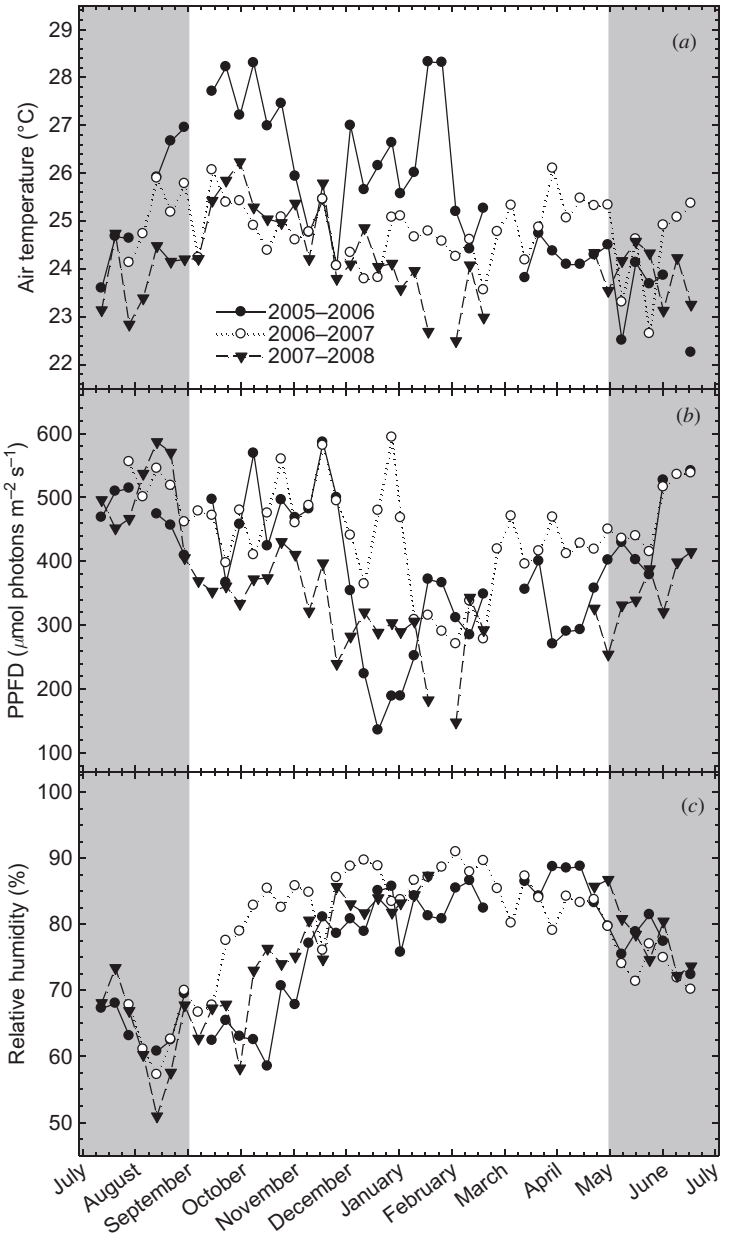

Figure 1. (*a*) Average air temperature, (*b*) photosynthetic photon flux density (PPFD), and (*c*) relative humidity calculated over 8 week intervals for the 2005–2006 (solid circles, solid lines), 2006–2007 (open circles, dotted lines), and 2007–2008 (inverted triangles, dashed lines) field seasons. The vertical shaded portions in each panel depict the dry season.

temperatures were the highest in 2005–2006 and the lowest in 2007–2008 until February, and after that, air temperature for 2006–2007 was higher than that for the other years (Figure 1(*a*)).

PPFD was highest during the dry season, when cloud cover was at a minimum, and lowest during the wet season as cloud cover increased (Figure 2(*b*)). Frequent cloud cover

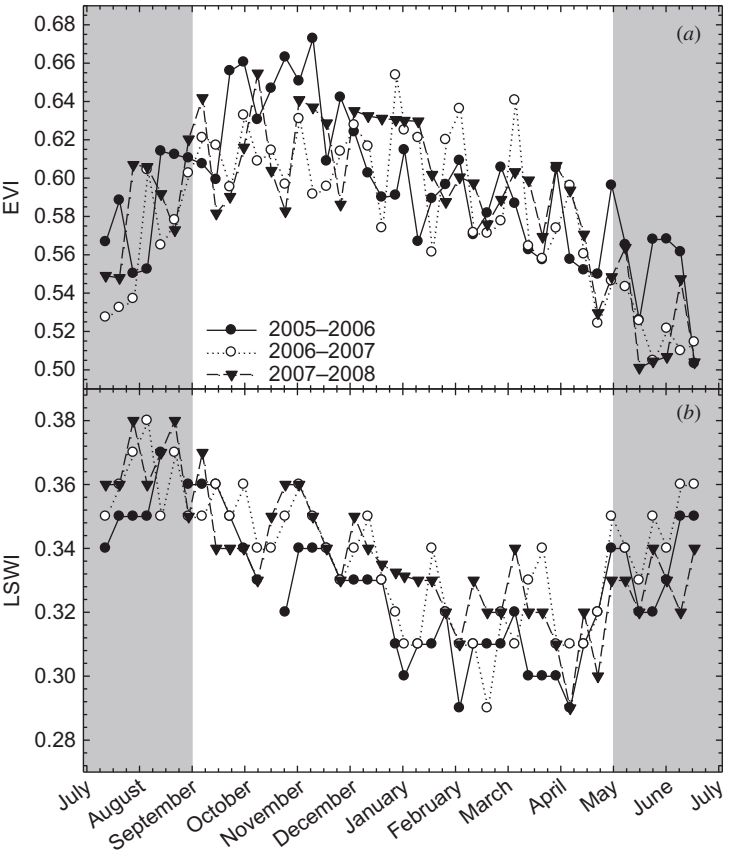

Figure 2. The (*a*) average enhanced vegetation index (EVI) and (*b*) land surface water index (LSWI) calculated over 8 week intervals for the 2005–2006 (solid circles, solid lines), 2006–2007 (open circles, dotted lines), and 2007–2008 (inverted triangles, dashed lines) field seasons. The vertical shaded portions in each panel depict the dry season.

also caused wet season PPFD values to be much more variable, and the lowest value of PPFD (~115 μmol photons m^{-2} s^{-1}) was observed in December 2005, which had one of the highest rainfall totals observed during the study period (Vourlitis et al. 2011).

Seasonal variations in RH were much less variable than temperature and PPFD over the study period (Figure 1(*c*)). The lowest values of RH (i.e. 50–60%) were observed during the dry season in late-August, whereas the peak values (80–90%) were observed in February during the peak of the wet season (Figure 1(*c*)).

3.2. *Seasonal variations in the EVI and LSWI*

Seasonal variations in the EVI were consistent from year to year, with low values during the dry season in May–September and peak values during the dry–wet season transition in November (Figure 2(*a*)). The increase in the EVI during the dry–wet season transition is consistent with the development of new leaves, increase in LAI, and increase in leaf nutrient concentration that typically occur as the rainy season ensues (Xiao et al. 2005; Asner and Martin 2008; Sanches et al. 2008). This pattern is more closely related to that

of savanna than of Amazonian forest (Ratana, Huete, and Ferreira 2005; Samanta et al. 2012), and reflects the importance of soil water availability, rather than radiation, in the seasonal phenology of leaf production in the semi-deciduous forest of the rainforest–savanna transition zone. In contrast, the LSWI displayed peaks in the dry season and a seasonal minimum during the wet season (February) and the wet–dry season transition in March–April (Figure 2(*b*)). The high values of LSWI during the dry season have been attributed to an increase in the proportion of young leaves, which have higher water content than older, senescent leaves (Roberts et al. 1998) and a high water-equivalent thickness of the upper canopy supplied by the deep root system (Xiao et al. 2005). However, the temporal trend in the LSWI was positively correlated with seasonal variations in leaf litter production (Figure 3(*a*)) and negatively correlated with seasonal variations in precipitation (Figure 3(*b*)) and soil water content (Figure 3(*c*)). Thus, as a land-surface water availability index, the LSWI appears to be negatively related with various water availability measures such as rainfall, soil water content, and RH ($r = -0.68$; $p < 0.001$; Figure 1(*c*)).

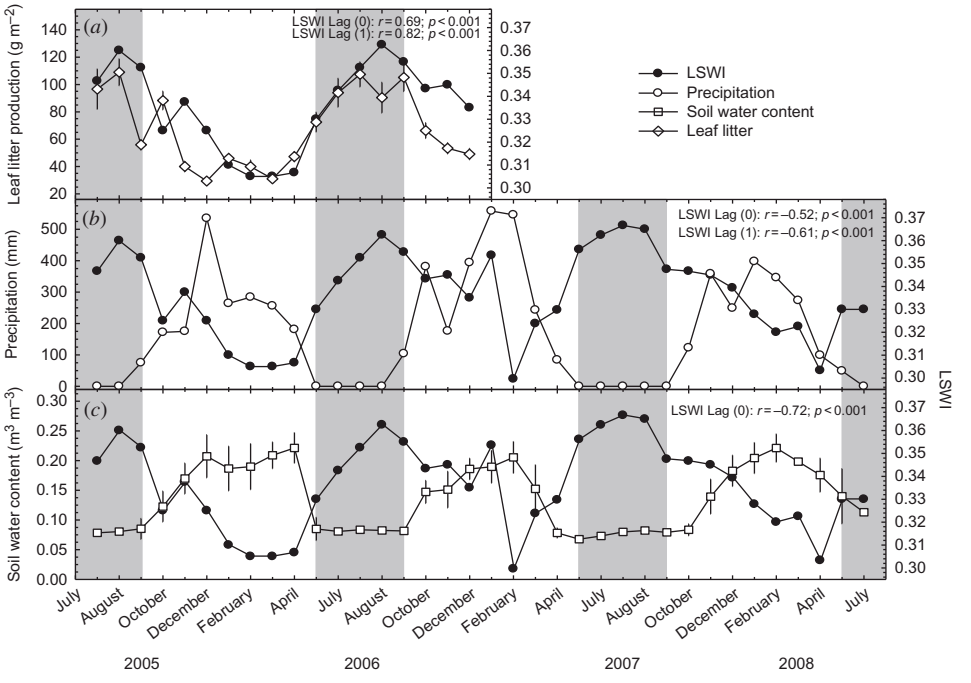

Figure 3. (*a*) Average (±se, $n = 10$) monthly leaf litter production (left-hand axis; open diamonds, solid line) and the land surface water index (LSWI; right-hand axis; solid circles, solid lines), (*b*) total monthly rainfall (left-hand axis; open circles, solid line) and the LSWI (right-hand axis; solid circles, solid lines), and (*c*) average (±sd; $n = 2$) soil water content in the upper 25 cm soil layer (left-hand axis; open circles, solid lines) and the LSWI (right-hand axis; solid circles, solid lines) during the study period. The vertical shaded portions in each panel depict the dry season. Also shown are the results from cross-correlation analysis (correlation coefficient (r) and the probability of a type-I error (p value)) between the LSWI and leaf litter production (*a*), precipitation (*b*), and soil water content (*c*) when the LSWI time series is either synchronized with the other time series (Lag (0)) or is lagged by 1 month with respect to the other time series (Lag (1)). Data for leaf litter production are from Sanches et al. (2008) and data for soil water content are from Vourlitis et al. (2008).

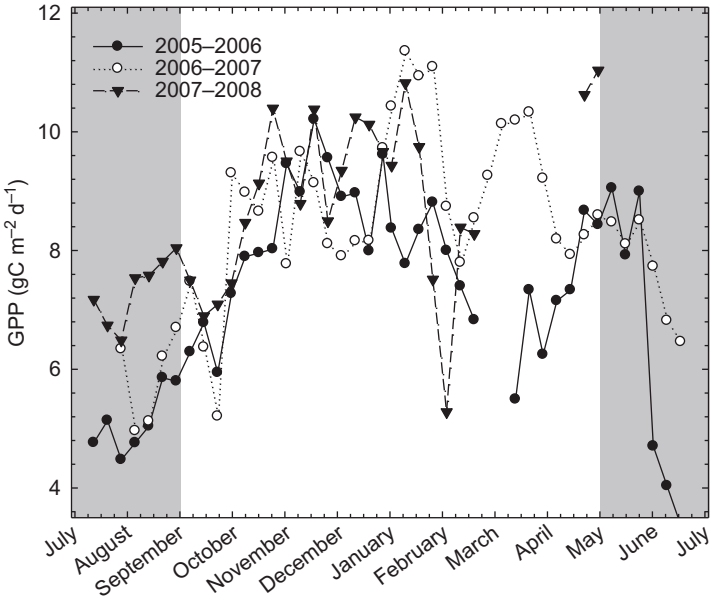

Figure 4. Average gross primary production (GPP) from eddy covariance measurements and models (Equation (2)) calculated over 8 week intervals for the 2005–2006 (solid circles, solid lines), 2006–2007 (open circles, dotted lines), and 2007–2008 (inverted triangles, dashed lines) field seasons. The vertical shaded portions in each panel depict the dry season.

Rates of GPP estimated from the eddy covariance data and the Michaelis–Menton light-use model (Equation (2)) exhibited lower values during the dry season and higher values during the wet season (Figure 4). These trends are coincident with seasonal variations in rainfall and soil water availability, and strong direct positive relationships between plant water potential and photosynthesis have been well-documented for tropical semi-deciduous forests (Miranda et al. 2005; Sendall, Vourlitis, and Lobo 2009) and savanna (Vourlitis and da Rocha 2010). However, variations in rainfall also indirectly affect GPP by affecting LAI (Poveda et al. 2001; Biudes et al. 2013), as was observed with the EVI (Figure 2(*a*); Vourlitis et al. 2011), nutrient uptake and availability (Myers et al. 1994), and VPD limitations on CO_2 uptake (Malhi et al. 1998; Araujo et al. 2002; Vourlitis et al. 2004, 2005, 2011).

3.3. *Analysis of the VPM*

Error analyses indicated that the standard VPM (Equations (5)–(10)) performed poorly in reconstructing the seasonal variations in GPP estimated from eddy covariance (Figure 5; Table 1). The standard VPM had the highest root mean square (RMSE) and mean absolute (MAE) errors, the lowest values (0.25–0.29) of Wilmont's index of agreement (*d*), and was not significantly correlated with the measured GPP (Table 1). The largest discrepancy between the measured and VPM-modelled GPP occurred during the dry seasons, when the modelled GPP was on average twice the measured values (Figure 5). Over each year, the standard VPM significantly overestimated average GPP by nearly 1.5 times during 2005–2006 and 2006–2007; however, differences between the VPM-derived GPP and that estimated from eddy covariance were not statistically significant during 2007–2008 (Table 2).

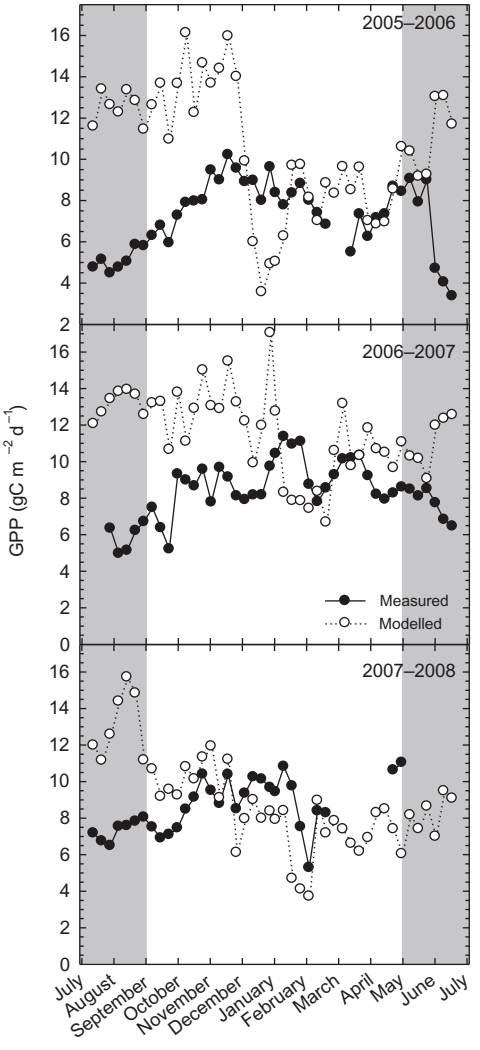

Figure 5. Average GPP derived from eddy covariance measurements (solid circles, solid lines) and the standard Vegetation Photosynthesis Model (VPM; open circles, dotted lines) calculated over 8 week intervals for the 2005–2006 (top panel), 2006–2007 (middle panel), and 2007–2008 (bottom panel) field seasons. The vertical shaded portions in each panel depict the dry season.

The reason for the discrepancy between the standard VPM and the measured values appeared to be due to the seasonal behaviour of the water availability scalar (W_{scalar}). Seasonal variations in the light-use efficiency (ε_g) exhibited minima during the dry season and maxima during the wet season (Figure 6(*a*)), which is consistent with other studies, highlighting the importance of rainfall and water availability on photosynthetic light-use efficiency (Miranda et al. 2005; Priante et al. 2004; Sendall, Vourlitis, and Lobo 2009; Vourlitis et al. 2001, 2004, 2005, 2011). The temperature scalar (T_{scalar}) would cause ε_g to increase during the wet–dry season transition (Figure 6(*b*)) as temperature increases and decrease during the wet season when temperature declines in response to frequent cloudiness (Figure 1(*a*)). The 28°C temperature optimum for canopy photosynthesis

Table 1. Error analysis of the gross primary production (GPP) estimates derived from the light-use efficiency model with different parameterizations of W_{scalar} compared to GPP estimated from eddy covariance. Error statistics include the root mean square (RMSE) and mean absolute (MAE) errors, Wilmont's statistic (d), the correlation coefficient (r) and the probability (p) of a statistically significant correlation, the intercept of the linear regression and the probability that the intercept is significantly different from zero ($p \neq 0$), and the slope of the linear regression and the probability that the slope is significantly different from unity ($p \neq 1$).

Period	Model	RMSE (gC m^{-2} day^{-1})	MAE	d	r (p)	Intercept ($p \neq 0$) (gC m^{-2} day^{-1})	Slope ($p \neq 1$)
2005–2006	Standard	5.11	4.23	0.29	−0.21 (NS)	13.32 (<0.001)	−0.38 (<0.001)
	RH	2.54	1.88	0.51	0.17 (NS)	6.16 (<0.001)	0.21 (<0.001)
	PPFD	1.92	1.50	0.50	0.21 (NS)	6.91 (<0.001)	0.13 (<0.001)
	RH + PPFD	1.54	1.28	0.62	0.49 (<0.001)	5.75 (<0.001)	0.25 (<0.001)
2006–2007	Standard	4.53	3.90	0.25	−0.30 (NS)	15.11 (<0.001)	−0.42 (<0.001)
	RH	3.55	2.70	0.42	0.40 (<0.005)	4.20 (<0.05)	0.76 (NS)
	PPFD	1.91	1.59	0.43	0.08 (NS)	7.22 (<0.001)	0.05 (<0.001)
	RH + PPFD	1.57	1.25	0.66	0.44 (<0.005)	4.98 (<0.001)	0.37 (<0.001)
2007–2008	Standard	3.63	3.00	0.25	−0.21 (NS)	13.05 (<0.001)	−0.41 (<0.001)
	RH	2.01	1.70	0.62	0.54 (<0.005)	1.97 (NS)	0.61 (<0.05)
	PPFD	1.56	1.19	0.61	0.35 (<0.05)	6.51 (<0.001)	0.28 (<0.001)
	RH + PPFD	1.28	0.97	0.76	0.60 (<0.001)	3.55 (<0.01)	0.57 (<0.005)
3 year	Standard	4.54	3.78	0.26	−0.22 (<0.05)	13.61 (<0.001)	−0.37 (<0.001)
	RH	2.84	2.13	0.50	0.32 (<0.001)	4.31 (<0.001)	0.54 (<0.005)
	PPFD	1.83	1.45	0.54	0.24 (<0.01)	6.74 (<0.001)	0.16 (<0.001)
	RH + PPFD	1.48	1.18	0.70	0.53 (<0.001)	4.88 (<0.001)	0.39 (<0.001)

Table 2. Mean (±95% CI) gross primary production from eddy covariance measurements (measured) and the light-use efficiency model using the standard W_{scalar} and those estimated from relative humidity (RH), photosynthetic photon flux density (PPFD), and a combined RH + PPFD model. Coefficients with an asterisk are not significantly different ($p < 0.05$) from the value estimated from eddy covariance (EC-Estimated).

	2005–2006	2006–2007	2007–2008
EC-Estimated	7.33 ± 0.51	8.25 ± 0.45	8.57 ± 0.52
Standard	10.52 ± 0.87	11.63 ± 0.65	8.88 ± 0.77*
RH	7.77 ± 0.58*	10.26 ± 0.67	7.15 ± 0.45
PPFD	7.60 ± 0.31*	7.59 ± 0.28*	8.69 ± 0.31*
RH + PPFD	7.60 ± 0.27*	7.94 ± 0.37*	7.85 ± 0.75*

(T_{opt}) and the behaviour of T_{scalar} are consistent with those reported for this and other tropical forests (Doughty and Goulden 2008; Vourlitis et al. 2011). However, because W_{scalar} is driven solely by variations in the LSWI (Equation (9)), which is negatively related to various water availability measures such as rainfall, soil water content, and RH (Figure 3), the standard version of W_{scalar} estimates little control of water availability on ε_g over the annual cycle (Figure 6(c)), although drought-induced declines in ε_g are well known from these seasonal forests (Miranda et al. 2005; Priante et al. 2004; Sendall, Vourlitis, and Lobo 2009; Vourlitis et al. 2001, 2004, 2005, 2011). In fact, water stress according to the standard W_{scalar} function is estimated to be relatively higher during the wet season than during the dry season (Figure 6(c)). Thus, in its current configuration, the VPM is incapable of reproducing GPP in these highly seasonal forests.

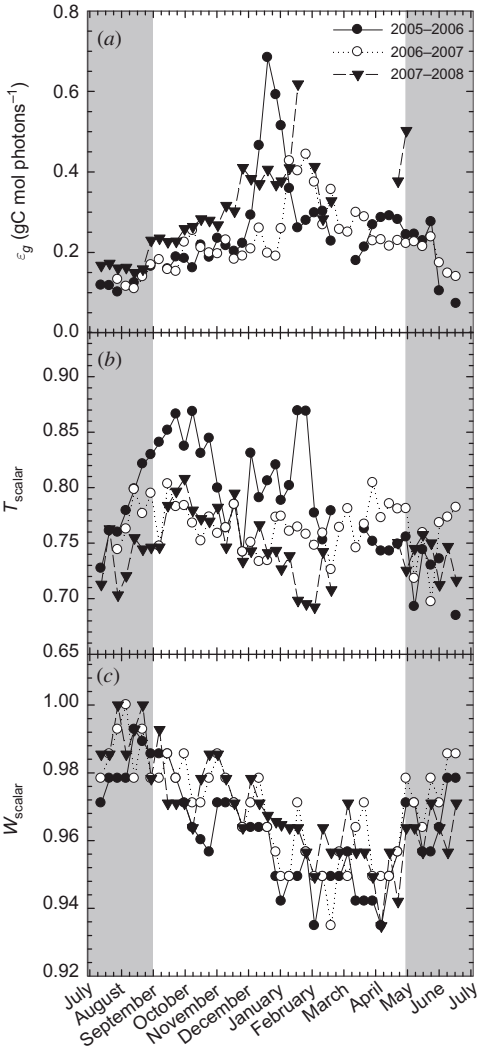

Figure 6. (*a*) Average light-use efficiency (ε_g) estimated from eddy covariance and Equation (2), (*b*) temperature scalar (T_{scalar}), and (*c*) the water availability scalar (W_{scalar}) from the standard VPM model calculated over 8 week intervals for the 2005–2006 (solid circles, solid lines), 2006–2007 (open circles, dotted lines), and 2007–2008 (inverted triangles, dashed lines) field seasons. The vertical shaded portions in each panel depict the dry season.

Following Vourlitis et al. (2011), new estimates of W_{scalar} were derived for this seasonal forest using measured values of RH and PPFD (Figure 7). These variables were used because ε_g has been observed to increase as a function of humidity (Vourlitis et al. 2011) and the potential for ε_g to decline as the average PPFD increases (Boardman 1977). We estimated a new W_{scalar} as a function of RH alone, PPFD alone, and RH and PPFD combined (Figure 8). The exponential RH function (Figure 7) ranged from 0.2 to 1.1 and followed a consistent seasonal trend from year to year with the lowest values in the dry season and dry–wet season transition and the highest values during December–April in the wet season (Figure 8(*a*)). The exponential PPFD function

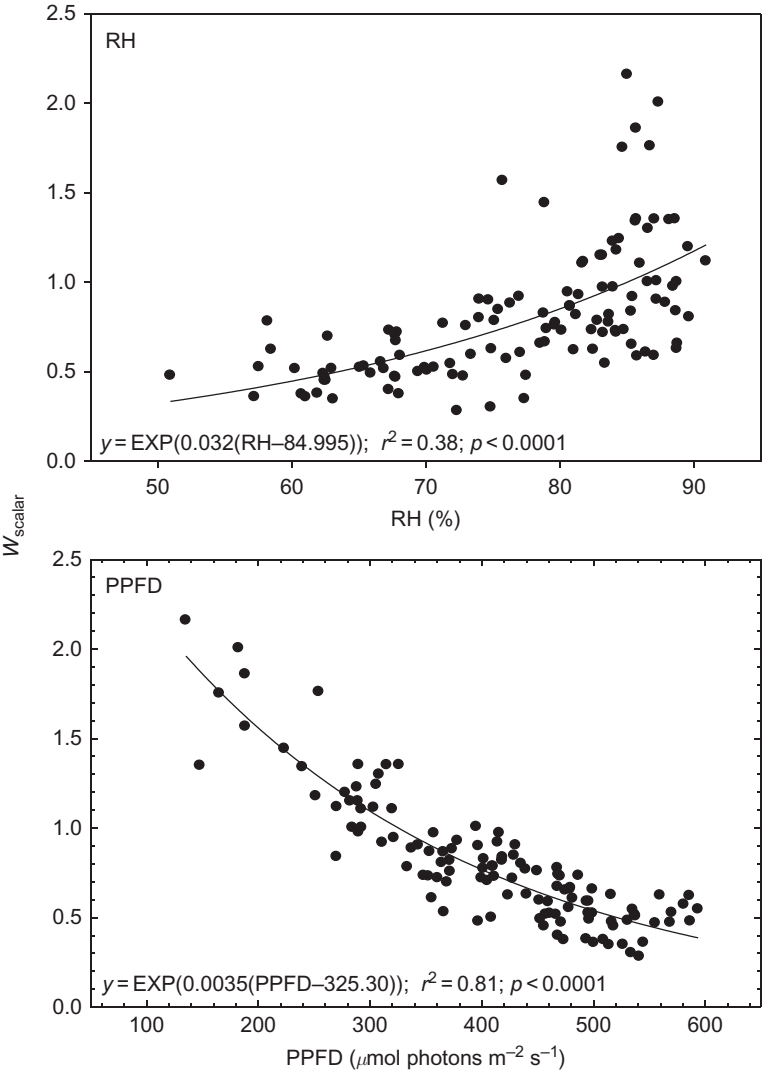

Figure 7. New W_{scalar} functions based on non-linear trends with relative humidity (top panel) and photosynthetic photon flux density (bottom panel). Estimates of W_{scalar} were derived by combining Equations (5)–(7) and solving for W_{scalar}.

(Figure 7) had a larger dynamic range than the RH function (0.4–1.9), and was more variable from year to year, reflecting the inter-annual variability in PPFD (Figure 8(*b*)). However, the PPFD function also exhibited lower values in the dry season and the highest values in the wet season. The combined function (RH + PPFD), which was a double exponential function, was almost identical to the PPFD-only function; however, the scalar values were slightly lower for the combined function (Figure 8(*c*)).

Error analyses indicated that the VPM with the new W_{scalar} functions performed significantly better than the standard model (Table 1). On average, the RMSE and MAE for the RH model were 50% of the standard model whereas the PPFD and RH + PPFD models had RMSE and MAE values that were 25–30% of the standard model (Table 1).

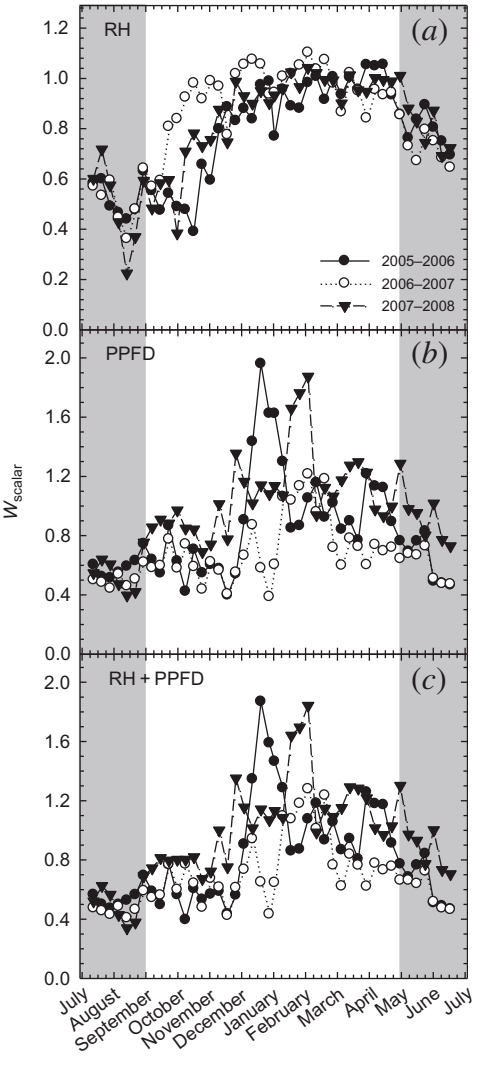

Figure 8. Time series of the new W_{scalar} functions based on relative humidity (*a*), photosynthetic photon flux density (*b*), and relative humidity and photosynthetic photon flux density combined (*c*), calculated over 8 week intervals for the 2005–2006 (solid circles, solid lines), 2006–2007 (open circles, dotted lines), and 2007–2008 (inverted triangles, dashed lines) field seasons. The vertical shaded portions in each panel depict the dry season.

Wilmont's index of agreement (*d*) was on average two times higher for the revised VPMs than for the standard model, and all of the correlations between the measured and modelled GPP values were positive and statistically significant, with the exception of the PPFD model during 2005–2006 (Table 1). Linear regression results with the modelled GPP as the dependent variable and measured GPP as the independent variable revealed that the RH model had substantially lower values for the *y*-intercept and higher values for the slope, indicating that modelled 8 week averages were closer to the measured values. The use of humidity as a sole variable for estimating the potential for water stress (actually VPD) is not without precedent, and forms the basis of adjusting the MODIS-derived GPP

estimates to spatial and temporal variations in water availability on a global scale (Mu et al. 2007).

In general, the PPFD and combined models had lower dynamic range than the RH model (Figure 9), and as a result, the *y*-intercept values were higher, and always significantly different from zero, and the slopes were lower and always significantly different from 1 (Table 1). However, the index of agreement (*d*) was higher for the PPFD and combined models, indicating a better fit to the measured values, which was also apparent when comparing the time series (Figure 9). In general, the RH model tended to significantly overestimate GPP during 2006–2007 and significantly underestimate GPP during 2007–2008 (Figure 9; Table 2). In contrast, the annual averages derived from the PPFD

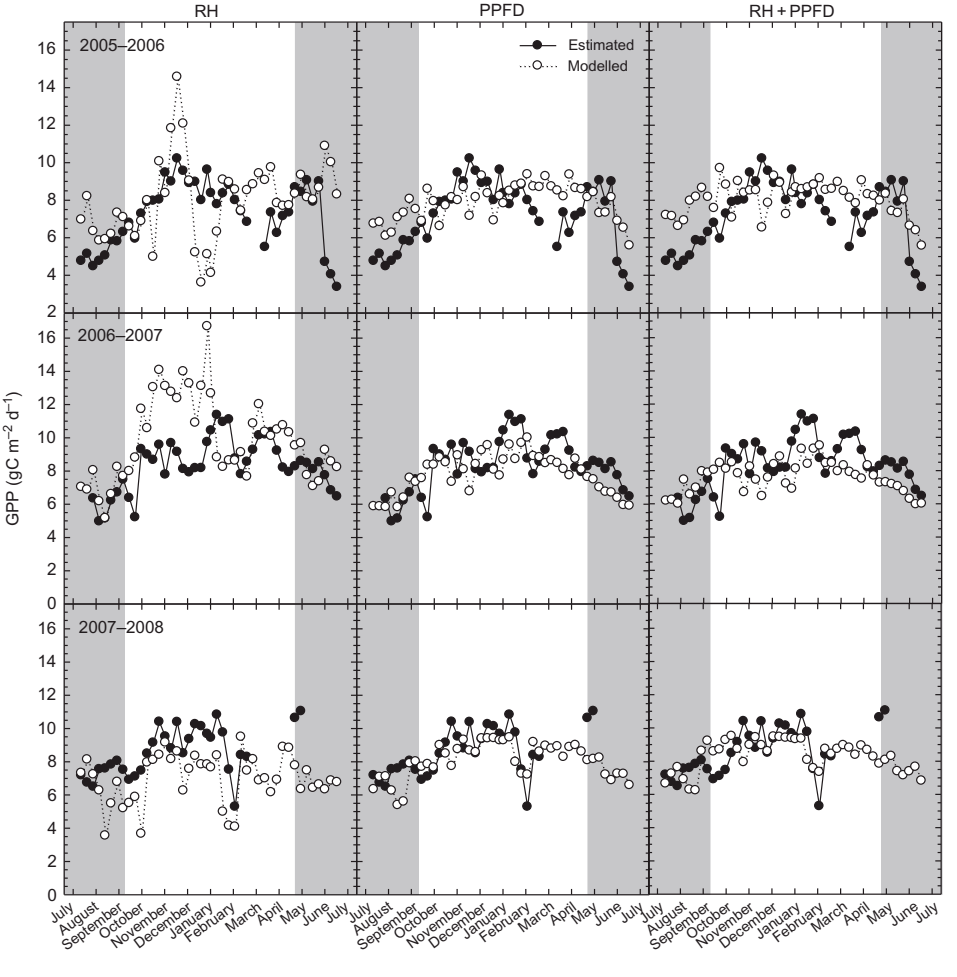

Figure 9. Average GPP derived from eddy covariance measurements (solid circles, solid lines) and the Vegetation Photosynthesis Model (VPM) with the new W_{scalar} function (open circles, dotted lines) based on relative humidity only (left-hand panels), photosynthetic photon flux density only (centre panels), and relative humidity and photosynthetic photon flux density combined (right-hand panels) calculated over 8 week intervals for the 2005–2006 (top panels), 2006–2007 (middle panels), and 2007–2008 (bottom panels) field seasons. The vertical shaded portions in each panel depict the dry season.

and combined models were not statistically different from the measured values for each year of the study period.

4. Conclusions

Estimates of tropical ecosystem GPP are required to quantify current and future rates of CO_2 uptake in response to land cover and climate change. Satellite data, and the spectral vegetation indices that are derived from them, are sensitive to temporal and spatial variations in LAI, phenology, and leaf chlorophyll content (Ratana, Huete, and Ferreira 2005; Huete et al. 2006; Samanta et al. 2012; Silva et al. 2013), but are limited by cloud cover during the wet season and biomass burning during the dry season when atmospheric clarity is impaired (Hird and McDermid 2009; Samanta et al. 2010; Zeilhofer et al. 2011). Satellite-based models are key tools for providing these estimates in remote and spatially extensive and complex areas. Many of these models use light-use efficiency approaches to estimate GPP as a function of the maximum light-use efficiency (ε_0), F_{PAR} (i.e. the EVI), and climate; however, these models also need realistic scalar functions to deal with climatic limitations (Xiao, Hollinger, et al. 2004; Mu et al. 2007; Wu, Chen, and Huang 2011). Here we found that the standard approach for estimating potential water limitations to GPP, based on an empirical relationship with LSWI, was inadequate for estimating the potential for drought limitations on GPP for a seasonal tropical forest in the south-central Amazon Basin. The standard W_{scalar} was not suitable in part because the seasonal pattern of the LSWI was negatively correlated with some of the key variables for water availability (precipitation, soil water content, and RH). These results highlight the importance of variable drivers of phenology (i.e. light and water availability) that extend across the Amazon Basin (Ratana, Huete, and Ferreira 2005), and the need to develop vegetation indices and/or algorithms for estimating GPP that capture these variable patterns of phenology (Silva et al. 2013). Based on previous research in seasonal tropical forest (Vourlitis et al. 2011), new functions of the water availability scalar (W_{scalar}) were derived from time series of RH and PPFD to provide estimates of GPP that were significantly more accurate than those derived from the standard approach. Variables such as RH (VPD) have been shown to be effective for characterizing spatial and temporal patterns of water stress over global scales (Mu et al. 2007). Whether these new functions perform equally well in water-stressed and unstressed tropical forests needs to be determined, but presumably unstressed ecosystems would have high cloud cover and humidity, which would minimize variations in W_{scalar}, and thus minimize variation in GPP to spatial and/or temporal variation in water availability.

Funding

Funding was provided by the US National Science Foundation-Office of International Science and Engineering (NSF-OISE), the Conselho Nacional de Desenvolvimento Científico e Tecnológico (CNPq), and the Fundação de Amparo à Pesquisa do Estado de Mato Grosso (FAPEMAT/PRONEX 823971/2009). Additional support was provided by Universidade Federal de Mato Grosso (UFMT) and the California State University, San Marcos (CSUSM).

References

Almeida, E. D. 2005. "Nitrogênio e fósforo no solo de uma floresta de transição Amazônia cerrado." MSc. thesis, Universidade Federal de Mato Grosso.

Anthoni, P. M., B. E. Law, and M. H. Unsworth. 1999. "Carbon and Water Vapor Exchange of an Open-Canopied Ponderosa Pine Ecosystem." *Agricultural and Forest Meteorology* 95: 151–168. doi:10.1016/S0168-1923(99)00029-5.

Araujo, A. C., A. D. Nobre, B. Kruijt, J. A. Elbers, R. Dallarosa, P. Stefani, C. von Randow, A. O. Manzi, A. D. Culf, J. H. C. Gash, R. Valentini, and P. Kabat. 2002. "Comparative Measurements of Carbon Dioxide Fluxes from Two Nearby Towers in a Central Amazonian Rainforest: The Manaus LBA Site." *Journal of Geophysical Research: Atmospheres* 107 (D20): 8090. doi:10.1029/2001JD000676.

Asner, G. P., and R. E. Martin. 2008. "Spectral and Chemical Analysis of Tropical Forests: Scaling from Leaf to Canopy Levels." *Remote Sensing of Environment* 112: 3958–3970. doi:10.1016/j.rse.2008.07.003.

Bernoux, M., M. S. Carvalho, B. Volkoff, and C. C. Cerri. 2002. "Brazil's Soil Carbon Stocks." *Soil Science Society of America Journal* 66: 888–896. doi:10.2136/sssaj2002.8880.

Biudes, M. S., N. G. Machado, V. H. M. Danelichen, M. C. Souza, G. L. Vourlitis, and J. S. Nogueira. 2013. "Ground and Remote Sensing-Based Measurements of Leaf Area Index in a Transitional Forest and Seasonal Flooded Forest in Brazil." *International Journal of Biometeorology.* doi:10.1007/s00484-013-0713-4.

Boardman, N. K. 1977. "Comparative Photosynthesis of Sun and Shade Plants." *Annual Review of Plant Physiology* 28: 355–377. doi:10.1146/annurev.pp.28.060177.002035.

da Rocha, H. R., A. O. Manzi, O. M. Cabral, S. D. Miller, M. L. Goulden, S. R. Saleska, N. R. Coupe, S. C. Wofsy, L. S. Borma, P. Artaxo, G. Vourlitis, J. S. Nogueira, F. L. Cardoso, A. D. Nobre, B. Kruijt, H. C. Freitas, C. von Randow, R. G. Aguiar, and J. F. Maia. 2009. "Patterns of Water and Heat Flux Across a Biome Gradient from Tropical Forest to Savanna in Brazil." *Journal of Geophysical Research* 114: GOOB12. doi:10.1029/2007jg000640.

Davidson, E. A., A. C. Araújo, P. Artaxo, J. K. Balch, I. F. Brown, M. M. C. Bustamante, M. T. Coe, R. S. DeFries, M. Keller, M. Longo, J. W. Munger, W. Schroeder, B. S. Soares-Filho, C. M. Souza, and S. C. Wofsy. 2012. "The Amazon Basin in Transition." *Nature* 481: 321–328. doi:10.1038/nature10717.

Doughty, C. E., and M. L. Goulden. 2008. "Seasonal Patterns of Tropical Forest Leaf Area Index and CO_2 Exchange." *Journal of Geophysical Research: Biogeosciences* 113 (G1): G00B06. doi:10.1029/2007JG000590.

Falge, E., D. Baldocchi, R. J. Olson, P. Anthoni, M. Aubinet, C. Bernhofer, G. Burba,G. Ceulemans, R. Clement, H. Dolman, A. Granier, P. Gross, T. Grunwald, D. Hollinger, N. O. Jensen, G. Katul, P. Keronen, A. Kowalski, C. T. Lai, B. E. Law, T. Meyers, J. Moncrieff, E. Moors, J. W. Munger, K. Pilegaard, U. Rannik, C. Rebmann, A. Suyker, J. Tenhunen, K. Tu, S. Verma, T. Vesala, K. Wilson, and S. Wofsy. 2001. "Gap Filling Strategies for Long Term Energy Flux Data Sets." *Agricultural and Forest Meteorology* 107: 71–77. doi:10.1016/S0168-1923(00)00235-5.

Ghil, M., M. R. Allen, M. D. Dettinger, K. Ide, D. Kondrashov, M. E. Mann, A. W. Robertson, A. Saunders, Y. Tian, F. Varadi, and P. Yiou. 2002. "Advanced Spectral Methods for Climatic Time Series." *Reviews of Geophysics* 40 (1): 3-1–3-41. doi:10.1029/2000RG000092.

Gloor, M., L. Gatti, R. Brienen, T. R. Feldpausch, O. L. Phillips, J. Miller, J. P. Ometto, H. Rocha, T. Baker, B. de Jong, R. A. Houghton, Y. Malhi, L. E. O. C. Aragão, J.-L. Guyot, K. Zhao, R. Jackson, P. Peylin, S. Sitch, B. Poulter, M. Lomas, S. Zaehle, C. Huntingford, P. Levy, and J. Lloyd. 2012. "The Carbon Balance of South America: A Review of the Status Decadal Trends and Main Determinants." *Biogeosciences* 9: 5407–5430. doi:10.5194/bg-9-5407-2012.

Golyandina, N., V. Nekrutkin, and A. Zhigljavsky. 2001. *Analysis of Time Series Structure: SSA and Related Techniques*. Boca Raton, FL: Chapman & Hall/CRC.

Golyandina, N., and E. Osipova. 2007. "The 'Caterpillar' – SSA Method for Analysis of Time Series with Missing Values." *Journal of Statistical Planning and Inference* 137: 2642–2653. doi:10.1016/j.jspi.2006.05.014.

Grace, J., Y. Malhi, J. Lloyd, J. Mcintyre, A. C. Miranda, P. Meir, and H. S. Miranda. 1996. "The Use of Eddy Covariance to Infer the Net Carbon Dioxide Uptake of Brazilian Rain Forest." *Global Change Biology* 2: 209–217. doi:10.1111/j.1365-2486.1996.tb00073.x.

Hernance, J. F., R. W. Jacob, B. A. Bradley, and J. F. Mustard. 2007. "Extracting Phenological Signals from Multiyear AVHRR NDVI Time Series: Framework for Applying High-Order Annual Splines." *IEEE Transactions on Geoscience and Remote Sensing* 45 (10): 3264–3276. doi:10.1109/TGRS.2007.903044.

Hird, J. N., and G. J. McDermid. 2009. "Noise Reduction of NDVI Time Series: An Empirical Comparison of Selected Techniques." *Remote Sensing of Environment* 113: 248–258. doi:10.1016/j.rse.2008.09.003.

Hollinger, D. Y., F. M. Kelliher, J. N. Byers, J. E. Hunt, T. M. McSeveny, and P. L. Weir. 1994. "Carbon Dioxide Exchange Between an Undisturbed Old-Growth Temperate Forest and the Atmosphere." *Ecology* 75: 134–150. http://www.jstor.org/stable/1939390.

Houghton, R. A. 2005. "Aboveground Forest Biomass and the Global Carbon Balance." *Global Change Biology* 11 (6): 945–958. doi:10.1111/j.1365-2486.2005.00955.x.

Huete, A., K. Didana, T. Miuraa, E. P. Rodrigueza, X. Gaoa, and L. G. Ferreirab. 2002. "Overview of the Radiometric and Biophysical Performance of the MODIS Vegetation Indices." *Remote Sensing of Environment* 83 (1–2): 195–213.

Huete, A. R., K. Didan, Y. E. Shimabukuro, P. Ratana, S. R. Saleska, L. R. Hutyra, W. Z. Yang, R. R. Nemani, and R. Myneni. 2006. "Amazon Rainforests Green-up with Sunlight in Dry Season." *Geophysical Research Letters* 33: L06045. doi:10.1029/2005GL025583.

Huete, A. R., H. Q. Liu, K. Batchily, and W. van Leeuwen. 1997. "A Comparison of Vegetation Indices Global Set of TM Images for EOSMODIS." *Remote Sensing of Environment* 59: 440–451. doi:10.1016/S0034-4257(96)00112-5.

Hutyra, L. R., J. W. Munger, S. R. Saleska, E. Gottlieb, B. C. Daube, A. L. Dunn, D. F. Amaral, P. B. de Camargo, and S. C. Wofsy. 2007. "Seasonal Controls on the Exchange of Carbon and Water in an Amazonian Rain Forest." *Journal of Geophysical Research-Biogeosciences* 112: G03008. doi:10.1029/2006JG000365.

Kim, Y., R. G. Knox, M. Longo, D. Medvigy, L. R. Hutyra, E. H. Pyle, S. C. Wofsy, R. L. Bras, and P. R. Moorcroft. 2012. "Seasonal Carbon Dynamics and Water Fluxes in an Amazon Rainforest." *Global Change Biology* 18: 1322–1334. doi:10.1111/j.1365-2486.2011.02629.x.

Laurance, W. F. 2006. "Forest-Climate Interactions in Fragmented Tropical Landscapes." In *Tropical Forests and Global Atmospheric Change*, edited by Y. Malhi, and O. L. Phillips, 31–40. Oxford: Oxford University Press.

Li, Z., G. Yu, X. Xiao, Y. Li, X. Zhao, C. Ren, L. Zhang, and Y. Fu. 2007. "Modeling Gross Primary Production of Alpine Ecosystems in the Tibetan Plateau Using MODIS Images and Climate Data." *Remote Sensing of Environment* 107: 510–519. doi:10.1016/j.rse.2006.10.003.

Losos, E. C., and E. G. Leigh Jr., eds. 2004. *Tropical Forest Diversity and Dynamism: Findings from a Large-Scale Plot Network*. Chicago, IL: University of Chicago Press.

Machado, L. A. T., H. Laurent, N. Dessay, and I. Miranda. 2004. "Seasonal and Diurnal Variability of Convection Over the Amazonia: A Comparison of Different Vegetation Types and Large Scale Forcing." *Theoretical and Applied Climatology* 78 (1–3): 61–77. doi:10.1007/s00704-004-0044-9.

Malhi, Y., A. Nobre, J. Grace, B. Kruijt, M. G. P. Pereira, A. Culf, and S. Scott. 1998. "Carbon Dioxide Transfer Over a Central Amazonian Rain Forest." *Journal of Geophysical Research: Atmospheres* 103: 31,593–31,612. doi:10.1029/98JD02647.

Marengo, J. A., C. A. Nobre, J. Tomasella, M. D. Oyama, G. S. de Oliveira, R. de Oliveira, H. Camargo, L. M. Alves, and I. F. Brown. 2008. "The Drought of Amazonia in 2005." *Journal of Climate* 21 (3): 495–516. doi:10.1175/2007JCLI1600.1.

McMillen, R. T. 1988. "An Eddy Correlation Technique with Extended Applicability to Non-Simple Terrain." *Boundary-Layer Meteorology* 43: 231–245. doi:10.1007/BF00128405.

Meir, P., D. B. Metcalfe, A. C. L. Costa, and R. A. Fisher. 2008. "The Fate of Assimilated Carbon During Drought: Impacts on Respiration in Amazon Rainforests." *Philosophical Transactions of the Royal Society B* 363: 1849–1855. doi:10.1098/rstb.2007.0021.

Miranda, E. J., G. L. Vourlitis, N. Priante-Filho, P. C. Priante, J. H. Campelo Jr., G. S. Suli, C. L. Fritzen, F. A. Lobo, and S. Shiraiwa. 2005. "Seasonal Variation in the Leaf Gas Exchange of Tropical Forest Trees in the Rain Forest-Savanna Transition of the Southern Amazon Basin." *Journal of Tropical Ecology* 21: 451–460. doi:10.1017/S0266467405002427.

Mu, Q., F. A. Heinsch, M. Zhao, and S. W. Running. 2007. "Development of a Global Evapotranspiration Algorithm Based on MODIS and Global Meteorology Data." *Remote Sensing of Environment* 111: 519–536. doi:10.1016/j.rse.2007.04.015.

Myers, R. J. K., C. A. Pahn, E. Cuevasi, U. N. Gunatilleke, and E. Bossard. 1994. "The Synchronisation of Nutrient Mineralization and Plant Nutrient Demand." In *The Biological Management of Tropical Soil Fertility*, edited by P. L. Woomerand, and M. J. Swift, 81–116. Chichester: John Wiley.

Myneni, R. B., W. Z. Yang, R. R. Nemani, A. R. Huete, R. E. Dickinson, Y. Knyazikhin, K. Didan, R. Fu, R. I. N. Juárez, S. S. Saatchi, H. Hashimoto, K. Ichii, N. V. Shabanov, B. Tan, P. Ratana, J. L. Privette, J. T. Morisette, E. F. Vermote, D. P. Roy, R. E. Wolfe, M. A. Friedl, S. W.

Running, P. Votava, N. El-Saleous, S. Devadiga, Y. Su, and V. V. Salomonson. 2007. "Large Seasonal Swings in Leaf Area of Amazon Rainforests." *PNAS* 104: 4820–4823. doi:10.1073/pnas.0611338104.

Nepstad, D. C., C. M. Stickler, B. Soares-Filho, and F. Merry. 2008. "Interactions Among Amazon Land Use, Forests and Climate: Prospects for a Near-Term Forest Tipping Point." *Philosophical Transactions of the Royal Society B* 363: 1737–1746. doi:10.1098/rstb.2007.0036.

Poveda, G., A. Jaramillo, M. M. Gill, N. Quiceno, and R. I. Mantilla. 2001. "Seasonally in ENSO-Related Precipitation, River Discharges, Soil Moisture, and Vegetation Index in Colombia." *Water Resources Research* 37: 2169–2178. doi:10.1029/2000WR900395.

Priante-Filho, N., G. L. Vourlitis, M. M. S. Hayashi, J. S. Nogueira, J. H. Campelo, P. C. Nunes, L. S. E. Souza, E. G., Couto, W. Hoeger, F. Raiter, J. L. Trienweiler, E. J. Miranda, P. C. Priante, C. L. Fritzen, M. Lacerda, L. C. Pereira, M. S. Biudes, G. S. Suli, S. Shiraiwa, S. R. Paulo, and M. Silveira. 2004. "Comparison of the Mass and Energy Exchange of a Pasture and a Mature Transitional Tropical Forest of the Southern Amazon Basin During a Seasonal Transition." *Global Change Biology* 10: 863–876. doi:10.1111/j.1529-8817.2003.00775.x.

Raich, J. W., E. B. Rastetter, J. M. Melillo, D. W. Kicklighter, P. A. Steudler, B. J. Peterson, A. L. Grace, B. Moore, and C. J. Vorosmarty. 1991. "Potential Net Primary Productivity in South America: Application of a Global Model." *Ecological Applications* 1: 399–429. doi:10.2307/1941899.

Ratana, P., A. R. Huete, and L. Ferreira. 2005. "Analysis of Cerrado Physiognomies and Conversion in the MODIS Seasonal–Temporal Domain." *Earth Interactions* 9 (3): 1–22. doi:10.1175/1087-3562(2005)0090001:AOCPAC2.0.CO;2.

Roberts, D. A., B. W. Nelson, J. B. Adams, and F. Palmer. 1998. "Spectral Changes with Leaf Aging in Amazon Caatinga." *Trees – Structure and Function* 12: 315–325. doi:10.1007/s004680050157.

Ruimy, A., P. G. Jarvis, D. D. Baldocchi, and B. Saugier. 1995. "CO_2 fluxes Over Plant Canopies and Solar Radiation: A Review." *Advances in Ecological Research* 26: 1–68. doi:10.1016/S0065-2504(08)60063-X.

Running, S. W., R. R. Nemani, F. A. Heinsch, M. Zhao, M. Reeves, and H. Hashimoto. 2004. "A Continuous Satellite-Derived Measure of Global Terrestrial Primary Production." *BioScience* 54: 547–560. doi:10.1641/0006-3568(2004)054[0547:ACSMOG]2.0.CO;2.

Running, S. W., P. E. Thornton, R. Nemani, and J. M. Glassy. 2000. "Global Terrestrial Gross and Net Primary Productivity from the Earth Observing System." In *Methods in Ecosystem Science*, edited by O. E. Sala, R. B. Jackson, and H. A. Mooney, 44–57. New York: Springer.

Saatchi, S. S., N. L. Harris, S. Brown, M. Lefsky, E. T. A. Mitchard, W. Salas, B. R. Zutta,W. Buermann, S. L. Lewis, S. Hagen, S. Petrova, L. White, M. Silman, and A. Morel. 2011. "Benchmark Map of Forest Carbon Stocks in Tropical Regions Across Three Continents." *PNAS* 108 (24): 9899–9904. doi:10.1073/pnas.1019576108.

Saleska, S., H. da Rocha, B. Kruijt, and A. Nobre. 2009. "Ecosystem Carbon Fluxes and Amazonian Forest Metabolism." In *Amazonia and Global Change, Geophysical Monograph Series*, edited by M. Keller, M. Bustamante, J. Gash, P. S. Dias, S. Saleska, H. Da Rocha, B. Kruijt, and A. Nobre, 389–408. Washington, DC: AGU.

Saleska, S. R., S. D. Miller, D. M. Matross, M. L. Goulden, S. C. Wofsy, H. R. da Rocha, P. B. de Camargo, P. Crill, B. C. Daube, H. C. de Freitas, L. Hutyra, M. Keller, V. Kirchhoff, M. Menton, J. W. Munger, E. H. Pyle, A. H. Rice, and H. Silva. 2003. "Carbon in Amazon Forests: Unexpected Seasonal Fluxes and Disturbance-Induced Losses." *Science* 302: 1554–1557. doi:10.1126/science.1091165.

Samanta, A., S. Ganguly, H. Hashimoto, S. Devadiga, E. Vermote, Y. Knyazikhin, R. R. Nemani, and R. B. Myneni. 2010. "Amazon Forests Did Not Green-up During the 2005 Drought." *Geophysical Research Letters* 37: L05401. doi:10.1029/2009GL042154.

Samanta, A., Y. Knyazikhin, L. Xu, R. E. Dickinson, R. Fu, M. H. Costa, S. S. Saatchi, R. R. Nemani, and R. B. Myneni. 2012. "Seasonal Changes in Leaf Area of Amazon Forests from Leaf Flushing and Abscission." *Journal of Geophysical Research* 117 (G1): G01015. doi:10.1029/2011JG001818.

Sanches, L., C. M. A. Valentini, O. B. P. Júnior, J. S. Nogueira, G. L. Vourlitis, M. S. Biudes, C. J. da Silva, P. Bambi, and F. A. Lobo. 2008. "Seasonal and Interannual Litter Dynamics of a Tropical Semi-Deciduous Forest of the Southern Amazon Basin, Brazil." *Journal of Geophysical Research* 113 (G4): G04007. doi:10.1029/2007JG000593.

Sendall, M. M., G. L. Vourlitis, and F. A. Lobo. 2009. "Seasonal Variation in the Maximum Rate of Leaf Gas Exchange of Canopy and Understory Tree Species in an Amazonian Semi-Deciduous Forest." *Brazilian Journal of Plant Physiology* 21: 65–74. doi:10.1590/S1677-04202009000100008.

Silva, F. B., Y. E. Shimabukuro, L. E. O. C. Aragão, L. O. Anderson, G. Pereira, F. Cardozo, and E. Arai. 2013. "Large-Scale Heterogeneity of Amazonian Phenology Revealed from 26-Year Long AVHRR/NDVI Time-Series." *Environmental Research Letters* 8 (2): 1–12. doi:10.1088/1748-9326/8/2/024011.

Valentini, C. M. A., L. Sanches, S. R. Paula, G. L. Vourlitis, J. S. Nogueira, O. B. Pinto Jr., and F. A. Lobo. 2008. "Soil Respiration and Aboveground Litter Dynamics of a Tropical Transitional Forest in Northwest Mato Grosso, Brazil." *Journal of Geophysical Research – Biogeosciences* 113 (G1): G00B10. doi:10.1029/2007JG000619.

Vermote, E. F., and S. Kotchenova. 2008. "Atmospheric Correction for the Monitoring of Land Surfaces." *Journal of Geophysical Research-Atmospheres* 113 (D23): D23S90. doi:10.1029/2007JD009662.

Vourlitis, G. L., and H. R. da Rocha. 2010. "Flux Dynamics in the Cerrado and Cerrado-Forest Transition of Brazil." In *Ecosystem Function in Global Savannas: Measurement and Modeling at Landscape to Global Scales*, edited by M. J. Hill, and N. P. Hanan, 97–116. Boca Raton, FL: CRC Press.

Vourlitis, G. L., F. A. Lobo, P. Zeilhofer, and J. S. Nogueira. 2011. "Temporal Patterns of Net CO_2 Exchange for a Tropical Semi-Deciduous Forest of the Southern Amazon Basin." *Journal of Geophysical Research* 116 (G3): G03029. doi:10.1029/2010JG001524.

Vourlitis, G. L., J. S. Nogueira, F. A. Lobo, K. M. Sendall, J. L. B. de Faria, C. A. A. Dias, and N. L. R. Andrade. 2008. "Energy Balance and Canopy Conductance of a Tropical Semi-Deciduous Forest of the Southern Amazon Basin." *Water Resources Research* 44 (3): W03412. doi:10.1029/2006WR005526.

Vourlitis, G. L., J. S. Nogueira, N. Priante-Filho, W. Hoeger, F. Railer, M. S. Biudes, J. C. Arruda, V. B. Capistrano, J. L. B. de Faria, and F. A. Lobo. 2005. "The Sensitivity of Diel CO_2 and H_2O Vapor Exchange of a Tropical Transitional Forest to Seasonal Variation in Meteorology and Water Availability." *Earth Interactions Journal* 9 (27): 1–23. doi:10.1175/EI124.1.

Vourlitis, G. L., N. Priante-Filho, M. M. S. Hayashi, J. S. Nogueira, F. T. Caseiro, and J. H. Campelo Jr. 2001. "Seasonal Variations in the Net Ecosystem CO_2 Exchange of a Mature Amazonian Transitional Tropical Forest (Cerradão)." *Functional Ecology* 15 (3): 388–395. doi:10.1046/j.1365-2435.2001.00535.x.

Vourlitis, G. L., N. Priante-Filho, M. M. S. Hayashi, J. S. Nogueira, F. T. Caseiro, F. Raiter, and J. H. Campelo Jr. 2004. "Effects of Meteorological Variations of the CO_2 Exchange of a Brazilian Transitional Tropical Forest." *Ecological Application* 14 (4): S89–S100. doi:10.1890/01-6005.

Wang, Z., X. Xiao, and X. Yan. 2010. "Modeling Gross Primary Production of Maize Cropland and Degraded Grassland in Northeastern China." *Agricultural and Forest Meteorology* 150 (9): 1160–1167. doi:10.1016/j.agrformet.2010.04.015.

Webb, E. K., G. I. Pearman, and R. Lenning. 1980. "Correction of Flux Measurements for Density Effects Due to Heat and Water Vapour Transfer." *Quarterly Journal of the Royal Meteorological Society* 106 (447): 85–100. doi:10.1002/qj.49710644707.

Wohlfahrt, G., C. Anfang, M. Bahn, A. Haslwanter, C. Newesely, M. Schmitt, M. Drosler, J. Pfadenhaeur, and A. Cernusca. 2005. "Quantifying Nighttime Ecosystem Respiration of a Meadow Using Eddy Covariance, Chambers and Modeling." *Agricultural and Forest Meteorology* 128 (3–4): 141–162. doi:10.1016/j.agrformet.2004.11.003.

Wu, C., J. M. Chen, and N. Huang. 2011. "Predicting Gross Primary Production from the Enhanced Vegetation Index and Photosynthetically Active Radiation: Evaluation and Calibration." *Remote Sensing of Environment* 115 (12): 3424–3435. doi:10.1016/j.rse.2011.08.006.

Wu, C., J. W. Monger, Z. Niu, and D. Kuang. 2010. "Comparison of Multiple Models for Estimating Gross Primary Production Using MODIS and Eddy Covariance Data in Harvard Forest." *Remote Sensing of Environment* 114 (12): 2925–2939. doi:10.1016/j.rse.2010.07.012.

Xiao, X., D. Hollinger, J. D. Aber, M. Goltz, E. A. Davidson, Q. Y. Zhang, and B. Moore III. 2004. "Satellite-Based Modeling of Gross Primary Production in an Evergreen Needleleaf Forest." *Remote Sensing of Environment* 89 (4): 519–534. doi:10.1016/j.rse.2003.11.008.

Xiao, X., Q. Zhang, B. Braswell, S. Urbanski, S. Boles, S. C. Wofsy, B. Moore III, and D. Ojima. 2004. "Modeling Gross Primary Production of Temperate Deciduous Broadleaf Forest Using

Satellite Images and Climate Data." *Remote Sensing of Environment* 91 (2): 256–270. doi:10.1016/j.rse.2004.03.010.

Xiao, X. M., S. Boles, J. Y. Liu, D. F. Zhuang, and M. L. Liu. 2002. "Characterization of Forest Types in Northeastern China, Using Multitemporal SPOT-4 VEGETATION Sensor Data." *Remote Sensing of Environment* 82 (2–3): 335–348. doi:10.1016/S0034-4257(02)00051-2.

Xiao, X. M., Q. Y. Zhang, S. Saleska, L. Hutyra, P. de Camargo, S. Wofsy, S. Frolkinga, S. Bolesa, M. Keller, and B. Moore III. 2005. "Satellite-Based Modeling of Gross Primary Production in a Seasonally Moist Tropical Evergreen Forest." *Remote Sensing of Environment* 94 (1): 105–122. doi:10.1016/j.rse.2004.08.015.

Zeilhofer, P., L. Sanches, G. L. Vourlitis, and N. L. R. Andrade. 2011. "Seasonal Variations in Litter Production and Its Relation with MODIS Vegetation Indices in a Semi-Deciduous Forest of Mato Grosso." *Remote Sensing Letters* 3 (1): 1–9. doi:10.1080/01431161.2010.523025.

Zhao, M., and S. W. Running. 2010. "Drought-Induced Reduction in Global Terrestrial Net Primary Production from 2000 Through 2009." *Science* 329 (5994): 940–943. doi:10.1126/science.1192666.